Degradation of the unstable *EP1* mRNA in *Trypanosoma brucei* involves initial destruction of the 3′-untranslated region

Henriette Irmer and Christine Clayton*

Zentrum für Molekulare Biologie Heidelberg, Im Neuenheimer Feld 282, D-69120 Heidelberg, Germany

ABSTRACT

Kinetoplastid protozoa regulate their gene expression primarily through control of mRNA degradation and translation. We describe here the degradation of three reporter mRNAs in *Trypanosoma brucei*. One mRNA had the 3′-untranslated region (3′-UTR) from the developmentally regulated *EP1* mRNA, which is abundant in the procyclic (tsetse fly) form of the parasite but is almost undetectable in the bloodstream form. This untranslated region includes a 26 nt U-rich sequence that causes extreme RNA instability in the bloodstream form. The two other RNAs, which are not developmentally regulated, had either the actin 3′-UTR, or a version of the *EP1* sequence lacking the 26 nt bloodstream-form instability element. All RNAs had poly(A) tails ~200 nt long, in both bloodstream and procyclic forms. Degradation of the two constitutively expressed mRNAs involved deadenylation and degradation by both 5′→3′ and 3′→5′ exonucleases. In contrast, in bloodstream forms, the 3′-end of the RNA bearing the bloodstream-form instability element disappeared very rapidly after transcription inhibition and partially deadenylated intermediates were not seen. The instability element may cause extremely rapid deadenylation, or it may be targeted by an endonuclease.

INTRODUCTION

African trypanosomes cause sleeping sickness in man and various diseases of domestic animals in sub-Saharan Africa. They multiply in the blood and tissue fluids of the mammal, and are transmitted from one host to the next by tsetse flies. Considerable adaptations in parasite morphology, surface composition and metabolism are required in order to survive in these disparate environments. For example, the bloodstream form of *Trypanosoma brucei* escapes the humoral immune response by antigenic variation, effected by frequent changes of the variant surface glycoprotein (VSG) (1). When the parasites transform to procyclic forms in the midgut of the tsetse fly, the VSG is replaced by proline-rich, acidic and repetitive EP/GPEET proteins. No *VSG* mRNA is detectable in procyclic forms and only minute amounts of *EP* mRNA have been found in bloodstream forms (2–4). Control of gene expression is crucial to parasite survival: expression of the EP/GPEET proteins in bloodstream forms would allow development of an effective immune response, and expression of developmentally regulated metabolic enzymes in the 'wrong' life-cycle stage can lead to cell death (5).

Nearly all trypanosomatid genes are found in very long polycistronic transcription units (6). There is no reproducible evidence for RNA polymerase II promoters or for developmental regulation of polymerase II transcription, and cotranscribed genes can have completely different expression patterns (3). After transcription, individual mRNAs are excised by a 5′ *trans* splicing reaction, which involves the addition of a short capped leader to the 5′-end of the RNA, and a coupled polyadenylation step (7–9). Thus capping of mRNAs is independent of the RNA polymerase used for transcription.

As a consequence of polycistronic transcription, nearly all developmental regulation of gene expression in trypanosomatids must be effected post-transcriptionally. The 5′-untranslated sequences do not play a major role in regulation, although weak 5′-splice sites result in constitutively low levels of mRNA and 5′-untranslated regions are involved in cell-cycle control of mRNA levels in the insect trypanosomatid *Crithidia fasciculata* (10). Most regulation is effected by sequences in the 3′-untranslated regions (3′-UTRs). This type of regulation was first shown for the *VSG* and *EP* genes (reviewed in 2,4,11,12) but in the meantime many examples of similarly regulated polymerase II transcripts have been reported (see for example 13–20). Both mRNA abundance and translation can be strongly regulated. The few relevant studies available have indicated that mRNA levels are controlled through regulated degradation (18,21–23).

Although nearly all protein-coding genes are transcribed by polymerase II, the *VSG* and *EP/GPEET* loci are transcribed by RNA polymerase I. Polymerase I transcription is about 10 times more active than transcription by RNA polymerase II (24), and initiation and/or elongation at the *EP/GPEET* and *VSG* loci is—in contrast to polymerase II—regulated by alterations in chromatin (for examples see 2,3,24–26). The *EP/GPEET* gene family consists of the *EP1* (gene encoding the EP1 protein, previously known as PARP or procyclin), *EP2*, *EP3* and *GPEET* genes (27). Transcription of the loci is only 10-fold less active in bloodstream forms than in procyclic forms (24), whereas the protein products are regulated at least

1000-fold. Post-transcriptional regulation is therefore extremely important (2,12). The 3′-UTRs of the *EP* and *GPEET* genes are quite divergent with the exception of a conserved 26mer and a 16mer stem–loop. The 16mer enhances translation in procyclic forms (28) and is not involved in developmental regulation. The sequences responsible for developmental regulation of mRNA abundance and translation are contained within the 26mer, an interrupted polyuridine tract (12,22,29), which is probably in a single-stranded conformation (30). The 26mer causes extreme instability of the *EP/ GPEET* mRNAs and represses their translation in bloodstream forms.

In both mammalian cells and the yeast *Saccharomyces cerevisiae*, sequences in the 3′-UTRs of mRNAs play a decisive role in regulation of mRNA decay. One important pathway of regulated mRNA degradation in yeast involves deadenylation followed by decapping and degradation by 5′→3′ exonucleases (31,32). In mutants of the 5′→3′ degradation pathway, degradation from the 3′-end can be observed (reviewed in 32). Although the basal components of the RNA degradation machinery are conserved from yeast to mammals (for examples see 33–35), mammals have some additional mechanisms. Degradation of several mRNAs is initiated by cleavage of a specific sequence within the 3′-UTR (36,37 and references therein), and proteins that bind such sequences can inhibit the degradation. Destabilising AU-rich elements (AREs) are found in the 3′-UTRs of many mammalian mRNAs involved in cell growth and differentiation (32). The mechanism of degradation promoted by these elements is controversial (32): it could proceed either via deadenylation and decapping (38,39) or be initiated by cleavage of the ARE by an endonuclease (40–42).

Despite the vital importance of RNA stability in the survival and pathogenicity of trypanosomes and Leishmanias, virtually nothing is known about the mechanisms of mRNA degradation in these organisms. Previous studies in trypanosomes have been restricted to reports showing that various inhibitors of protein synthesis increase the abundance of *EP* mRNAs in bloodstream forms (43–45). These studies have generally been interpreted as implying that degradation is mediated by an unstable protein. However, because very few mRNAs have been studied in this way, it is not clear whether the postulated unstable protein is specific for particular mRNAs, or part of the general mRNA degradation machinery. The mechanisms of translation control are completely unknown. To understand regulated mRNA turnover in trypanosomes, and to define the effector molecules, it is necessary to define the pathways involved in constitutive and regulated degradation. In this paper we compare the pathway of *EP1* 3′-UTR-mediated mRNA degradation with that mediated by a 3′-UTR from the actin (*ACT*) mRNA, which is not developmentally regulated.

MATERIALS AND METHODS

Trypanosome culture and transfection

Bloodstream and procyclic trypanosomes (MiTat 1.2) were cultured and transfected, and CAT assays performed as described (22,46). Neomycin-resistant bloodstream trypanosomes expressing T7 polymerase were generated by transfecting 10^7 trypanosomes with 10 μg plasmid DNA linearised within β-tubulin targeting sequence, and selected with 15 μg/ml

G418. These trypanosomes were transfected with plasmids that were linearised within an rRNA targeting sequence, selected with 15 μg/ml hygromycin and cloned by limiting dilution.

Plasmid constructs

The plasmid encoding T7 polymerase was kindly provided by E. Wirtz (pLew13) (47). Plasmids for stable transfection were based on pLew82 (47). These carried a T7 promoter, and chloramphenicol acetyltransferase (*CAT*) and hygromycin resistance (*HYG*) cassettes. Downstream of the *CAT* gene were placed various 3′-UTRs, followed by a region from 5′ of the actin (*ACT*) gene that ensures *trans* splicing of the *HYG* mRNA and polyadenylation of the preceding *CAT* mRNA (22). The initial plasmids carried the following 3′-UTRs downstream of the *CAT* gene: *CAT-EP1* (pHD 774) *CAT-ACT* (pHD 789) *CAT-ep1Δ26* (pHD 775). Variants of these plasmids bearing a ribosomal RNA promoter instead of a T7 promoter were also tested (in cells lacking T7 polymerase).

Secondary structures were introduced by cloning G_{30} oligos with restriction overhangs into available or newly created restriction sites. All constructs were sequenced in both directions (TopLab, München, Germany). In nearly every case, the sequence terminated in the middle of a G_{30} or C_{30} tract, so the size of the complete insertion was confirmed by restriction digestion. The constructs created were as follows, where *G* indicates that the resulting mRNA contains G_{30} and *GC* indicates that $G_{30}C_{30}$ is present at the indicated positions: *CAT-ep1-G-26* (with G_{30} inserted at position 120 in the 3′-UTR, preceding the 26mer, pHD 879); *CAT-GC-EP1* (pHD 921); *5′-G-CAT-EP1* (pHD 874); *CAT-EP1-G* (with G_{30} inserted at position 180 in the 3′-UTR, after the 26mer, pHD 891); *5′-G-CAT-GC-EP1* (pHD 922); *CAT-GC-ACT* (pHD 1110); *5′-G-CAT-ep1Δ26* (pHD 873); *CAT-G-ep1Δ26* (pHD 1109). These constructs are illustrated in Figure 4. Additional, similar constructs bearing insertions of 18 G residues, or six *Bam*HI linkers, were initially tested but yielded no intermediates; however, these were never analysed using RNase H.

RNA preparation and manipulation

Total RNA was isolated using peqGoldTrifast (peqLab). RNA from 4×10^7 cells was separated on formaldehyde gels and blotted onto Nytran membrane (Schleicher and Schuell). In turnover experiments, ^{32}P-labelled probes were used and bands quantitated using a PhosphorImager (Molecular Dynamics). For *in vitro* transcription of *CAT* constructs, plasmids were cut with *Spe*I and transcribed according to the manufacturer's instructions, then either viewed by direct staining or blotted and detected with specific probes.

RNase H assays were carried out incubating 250 μmol oligos with 10–20 μg total RNA and RNase inhibitor (Rnasin, Stratagene) for 10 min at 45°C. RNase H (1 U; Roche, Mannheim) and RNase H buffer (50 mM Tris–HCl, pH 7.4, 10 mM $MgCl_2$, 80 mM KCl, 1 mM DTT) were added and the mixture was incubated for 2 h at 37°C followed by a precipitation step. The RNA was run on 5% denaturing polyacrylamide gels followed by semi-dry blotting on Nytran membrane. mRNA was detected using digoxygenin-labelled RNA probes as described by the manufacturer (Roche, Mannheim).

RESULTS

Degradation of *CAT* mRNAs synthesised by T7 polymerase

In our previous work on post-transcriptional regulation in trypanosomes, we studied the degradation of *CAT* mRNAs bearing different 3′-UTRs, produced from transgenes integrated into the trypanosome genome and transcribed by RNA polymerase II. Actinomycin D was added to trypanosome cultures, to inhibit mRNA synthesis, and the levels of RNAs were measured at various times after drug addition by northern blotting. In bloodstream-form trypanosomes, *CAT* RNA bearing the 3′-UTR from the *EP1* gene (*CAT-EP1* RNA) was barely detectable and had a half-life of 5–7 min (22). An mRNA with the 3′-UTR from the *ACT* gene (*CAT-ACT* mRNA) served as an unregulated control; after actinomycin D addition, the RNA level rose for the first 10 min, then diminished with a half-life of ~20 min. We do not know why the mRNA levels rise immediately after actinomycin D addition, but this is extremely reproducible and has been seen in similar experiments with *Leishmania chagasi* (see fig. 4 in ref. 48). An RNA bearing an *EP1* 3′-UTR with a deletion of the 26mer (*CAT-ep1Δ26*) behaved exactly like the *CAT-ACT* mRNA. Similar half-lives were observed after addition of sinefungin, which inhibits mRNA processing in trypanosomes because it inhibits cap methylation on the spliced leader RNA. In procyclic forms, the *CAT-EP1* RNA, like the *EP1* RNA, was much more stable than the *ACT* or *CAT-ACT* RNAs. These latter mRNAs, like other mRNAs that are expressed at a constant level throughout the life cycle, were slightly more stable in procyclic forms than in bloodstream forms. This compensates for the fact that procyclic trypanosomes have a greater volume than bloodstream forms, and a slightly longer division time.

In order to study the degradation mechanism, we needed cell lines expressing more mRNA from the integrated *CAT* transgenes than can be obtained using RNA polymerase II. Initially, we re-engineered the plasmids to ensure transcription by trypanosome RNA polymerase I, which is approximately 10 times as active as polymerase II (24). Then we replaced the rRNA promoter with a bacteriophage T7 promoter, and transfected the plasmids into trypanosomes expressing T7 RNA polymerase (47,49). The relative mRNA levels and CAT activities obtained from the new constructs are illustrated in Figure 1. Maximum expression was obtained when the integrated transgenes were transcribed by T7 polymerase. Despite the high expression, however, the control by 3′-UTRs was retained. In our previous paper, where the *CAT* constructs were transcribed by RNA polymerase II, the levels of *CAT-EP1* and *CAT-ep1Δ26* RNAs were ~9 and 34% relative to the *CAT-ACT* mRNA (22) and relative CAT activities were similar. The mRNAs expressed using T7 polymerase were present in the same ratios, but rather more translation of *CAT-ep1Δ26* was seen (Fig. 1).

We next checked the kinetics of RNA degradation in the T7 polymerase lines. It was important to confirm that the excess production of 26mer-containing RNA had not saturated the regulation mechanism. Bloodstream trypanosomes expressing *CAT-ACT*, *CAT-EP1* and *CAT-ep1Δ26* mRNAs from the T7 promoter were treated with actinomycin D and the levels of
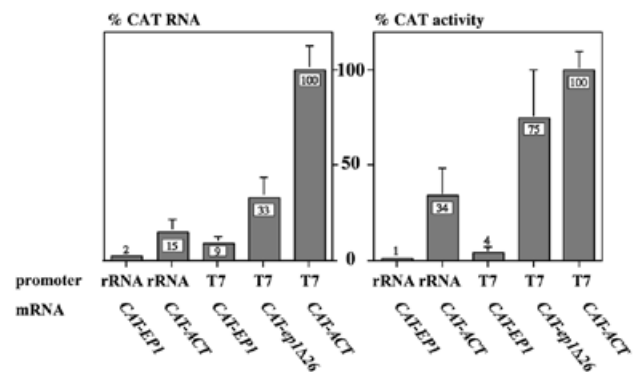

Figure 1. Levels of mRNAs influenced by the RNA polymerase used for transcription, and the nature of the 3′-UTR. The plasmids used were designed for integration into the silent *RRNA* spacer, and had a T7 promoter (P_{T7}) or ribosomal RNA promoter (P_{RRNA}) preceeding a 5′-UTR (*trans* splicing acceptor site) and the *CAT* gene. The *CAT* gene was followed by various 3′-UTRs: actin (*ACT*); *EP1*; and a derivative of *EP1* that lacked the 26mer instability element (*ep1Δ26*). The different 3′-UTRs were followed by a cassette allowing selection of permanent trypanosome transformants: a splice acceptor, the *HYG* gene (hygromycin resistance) and an actin 3′-UTR. The graphs show relative levels of *CAT* mRNA and CAT activity in bloodstream trypanosomes stably transformed with different constructs. The nature of the promoter, and of the 3′-UTR following the *CAT* gene, are shown beneath the columns. Values are expressed as a percentage, with the mean for the *CAT-ACT* construct with a T7 promoter set at 100%. The error bars show the standard deviation of at least three independent measurements.

RNA measured by northern blotting. The very stable *VSG* mRNA (21) was treated as a loading control. Results are shown in Figure 2. The RNAs behaved exactly as previously described. The *CAT-ACT* and *CAT-ep1Δ26* mRNAs first accumulated then were degraded with half-lives of ~15 min, and the *CAT-EP1* mRNA disappeared with a half-life of ~7 min. Importantly, however, the *CAT-EP1* mRNA was now detectable for long enough to allow detection of degradation intermediates.

Cell lines were also generated with procyclic trypanosomes using the same constructs. The stabilities of the resulting mRNAs were again similar to those previously measured for procyclic forms (22), with half-lives of 1–2 h for all 3′-UTRs.

Fate and length of the poly(A) tail during degradation

To find out which ends of the test mRNAs were attacked first by the degradation machinery, we needed to separate the 3′-end from the 5′-end. This was done by cleaving the mRNAs into three pieces: a 5′ fragment, a central piece and a 3′ fragment. To achieve this, the RNA samples were incubated with two oligonucleotides, specific for different parts of the *CAT* gene, together with RNase H. The RNase H cleaved each *CAT* RNA at the sites of oligonucleotide hybridisation, giving three fragments which are designated A, B and C in Figure 3A. The largest fragment (A in Fig. 3A) contained the 3′ portion of the *CAT* gene attached to the 3′-UTR and the poly(A) tail. The next largest fragment (B) was the 5′ portion of the *CAT* gene attached to the 5′-UTR and the spliced leader, and the smallest fragment (C) was the central portion of the *CAT* gene. To determine the length of the poly(A) tail, we included oligo d(T) in the RNase H incubations. This resulted in deadenylation of
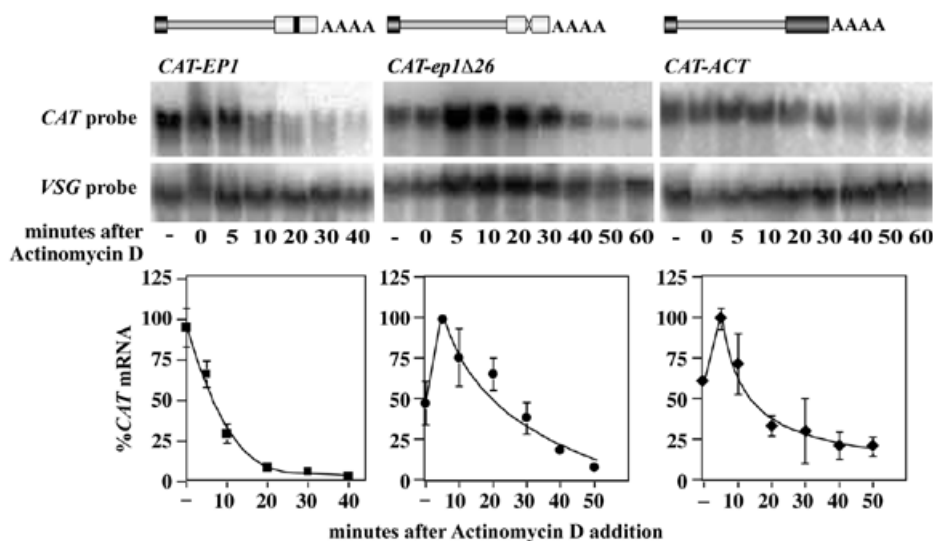
Figure 2. Degradation kinetics of the *CAT* mRNAs produced by T7 polymerase. Actinomycin D was added to 10 µg/ml at time 0 and RNA prepared at the times indicated. The first time point (lane indicated –) is cells without actinomycin D and the time = 0 lane is cells placed on ice and centrifuged immediately after addition of actinomycin D. The upper panels are typical northern blots, hybridised with the probes shown. Within each panel, all lanes are from the same exposure, but some lanes were deleted from the centre of the *CAT-EP1* and *CAT-ep1Δ26* illustrations. The *VSG* mRNA is very stable in bloodstream trypanosomes so was used as a loading control. The lower panels show the relative mRNA levels, with the highest point taken as 100%. The quantitated results are expressed as the mean and standard deviation of at least three independent experiments.

the 3′ fragment. The sizes and relative abundances of the fragments were analysed by denaturing polyacrylamide gel electrophoresis and blot hybridisation (Fig. 3B).

In yeast and mammals, mRNA degradation is frequently initiated by degradation of the poly(A) tail. To see if this was true in trypanosomes, we inhibited transcription using actinomycin D as before, and isolated RNA at different time points. The mRNAs were then cleaved into three pieces as described. Experiments were performed at least four times on each RNA; representative results are shown in Figure 3B. Often, additional fragments were present in amounts that varied considerably between experiments; these are marked with asterisks in the figures. After blot hybridisation with specific fragments of the *CAT* gene, and testing a variety of incubation conditions (data not shown), we concluded that these were mainly products of incomplete RNase H cleavage.

The steady-state lengths of the poly(A) tails on all three RNAs were 150–200 nt, as judged by comparing the size of fragment A in the zero time-point lane without oligo d(T) with the size of fragment A incubated with oligo d(T). (These lanes are on the extreme right of the panels in Fig. 3B.) The degradation pattern of the *CAT-ACT* and *CAT-ep1Δ26* mRNAs (centre and right-hand panels in Fig. 3B) followed a pattern indicating that degradation is preceded by deadenylation. After actinomycin D addition, the sizes of the 5′ (B) and central (C) fragments remained constant for 40 min, although their abundance decreased. In contrast, the 3′ fragment (A) gradually became shorter. The reduction in size can be seen in Figure 3B by comparing the migration of the 3′ fragment A at the 40 min time point with the migration of deadenylated fragment A and fragment A at time = 0. Deadenylation was more clearly seen when the gel electrophoresis was prolonged to improve resolution of the longer fragments (Fig. 3C, see the panels for *CAT-ep1Δ26* and *CAT-ACT*).

The *CAT-EP1* mRNA degradation pattern in bloodstream forms was clearly different from that of the other two transcripts (Fig. 3B and C). The full-length 3′ fragment A disappeared rapidly. Its disappearance preceded the disappearance of the other two fragments and there was no sign of deadenylation intermediates. This was also true 5 min after actinomycin D addition (not shown). This implied that degradation was initiated by extremely rapid destruction of the 3′-UTR, possibly through an endonuclease cleavage followed by 3′→5′ digestion. Throughout the incubation, however, there was a faint band that corresponded in length to the fully deadenylated species (seen clearest in Fig. 3C, *CAT-EP1* bf). This result suggested to us that a very minor portion of the *CAT-EP1* mRNA was subject to rapid deadenylation.

When we repeated these experiments in procyclic forms, we saw that the degradation of the *CAT-EP1* mRNA now followed the same pathway as that for the *CAT-ACT* and *CAT-ep1Δ26* mRNAs (Fig. 3C, *CAT-EP1* pro, and data not shown). As previously shown, the *CAT-EP1* mRNA was much more stable in procyclic than in bloodstream forms. The length of the poly(A) tail on *CAT-EP1* mRNA was not developmentally regulated (compare the bf and pro lanes at zero time), but deadenylation was clearly visible after transcription inhibition. Thus the rapid destruction of the *EP1* 3′-UTR correlated with mRNA instability, while more stable mRNAs were degraded by a more classical pathway involving deadenylation.

The direction of regulated degradation

As already noted, a possible mechanism for *EP1* mRNA degradation in bloodstream trypanosomes would be an endonuclease cleavage at or near the 26mer. We therefore tried to find specific cleavage products by RNase protection assays. Despite considerable efforts, using a variety of probes and including clear positive controls, the results were consistently
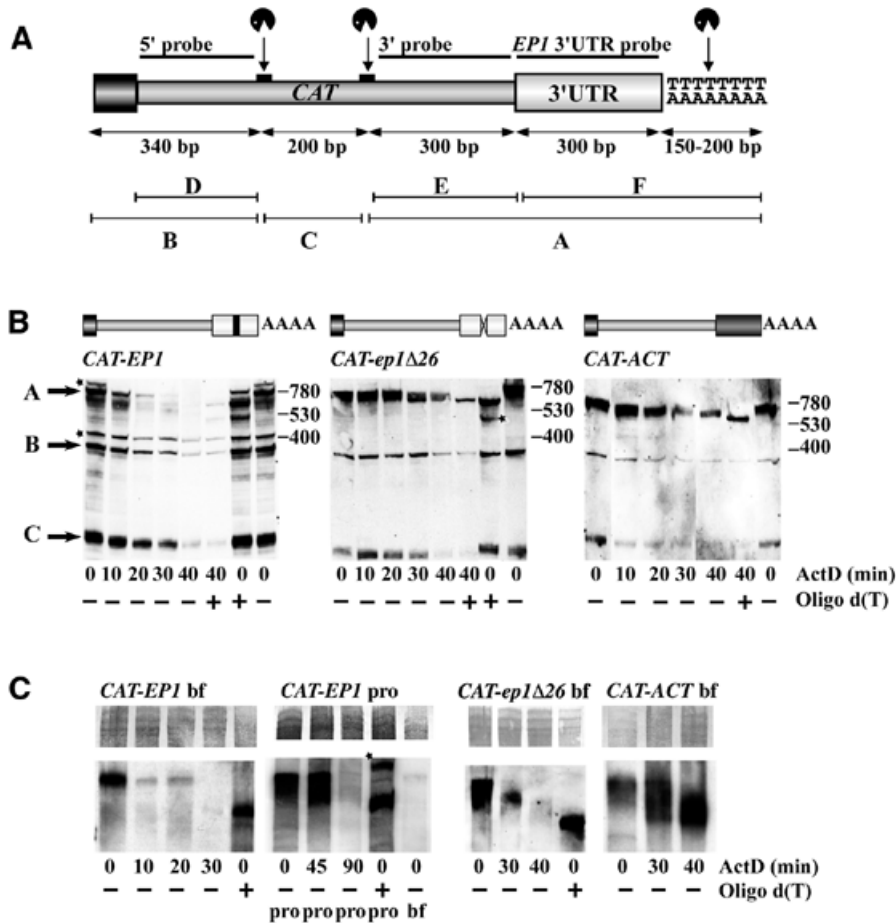
Figure 3. Differential degradation kinetics of the 3′- and 5′-ends of the mRNAs. (**A**) Diagram of a generic *CAT* mRNA, showing the sites of RNase H cleavage after addition of targeted oligonucleotides. The fragments illustrated in (B) and (C), and also those seen in Figure 5 together with the specific probes, are indicated. (**B**) Northern blots displaying the mRNA fragments. RNA was isolated from the cell lines at various times after addition of actinomycin D, as in Figure 2. The RNA was subsequently digested with RNase H and specific oligonucleotides, and the resulting fragments separated on denaturing polyacrylamide gels. The identity of the bands was confirmed by hybridisation with specific probes (see Figure 5); bands marked * are partial digestion products. In (C), a methylene blue stain of the blot is shown above to indicate loading. (**C**) The experiment shown in (B) was repeated but the gel was run much longer, to increase resolution of the 3′-end fragment A. This better illustrates deadenylation of the *CAT-ACT* and *CAT-ep1_26* mRNAs, and also shows that the *CAT-EP1* mRNA is deadenylated in procyclic forms (pro), but not in bloodstream forms (bf). The panels above the blots show the stained rRNAs.

negative (not shown) (50). This result has two possible explanations. First, there may indeed be no cleavage in or near the 26mer, but it is also possible that cleavage occurs and the products are very rapidly degraded.

As an alternative we adopted an approach that had already successfully been used in yeast (31,51) and in *Chlamydomonas reinhardtii* (52). Here, the direction of degradation was determined by examining the fate of modified transcripts containing poly(G) tracts, which form stable secondary structures that impede the progress of exonucleases and lead to the accumulation of stable intermediates. We inserted secondary structures into the *CAT* constructs, and made transgenic bloodstream trypanosomes. The relevant constructs are illustrated in Figure 4. The minimal sequence inserted was G_{30} (indicated by G in the plasmid names), but some plasmids contained $G_{30}C_{30}$ (indicated by GC in the plasmid names). To detect 5′→3′ exonuclease activity, G_{30} was inserted immediately preceding the *CAT* gene (5′-G-CAT-EP1, construct 5; 5′-G-CAT-ep1Δ26, construct 4). Similarly, to detect 3′→5′ exonuclease action,

secondary structure was inserted at the junction between the *CAT* gene and the 3′-UTR (*CAT-GC-EP1*, construct 8; *CAT-GC-ACT*, construct 11; *CAT-G-ep1Δ26*, construct #10). In order to look for endonuclease cleavage in the *EP1* 3′-UTR, structures were also inserted either immediately preceding the 26mer (*CAT-EP1-G-26*, construct 6) or within the 16mer stem–loop, downstream of the 26mer (*CAT-EP1-26-G*, construct 7). Selected constructs were also transfected into procyclic forms.

We intially looked for intermediates by northern blotting. The blot at the foot of Figure 4 displays RNA from each line, with each lane number corresponding to the number of the transfected construct. The relative abundances of the starting RNAs are clearly seen (lanes 1–3). With one exception, the structures did not reproducibly influence the mRNA abundance. (Compare for example lanes 11 and 3, and lanes 1, 5, 7, 8 and 9.) The exception was the mRNA in which a poly(G) had been inserted immediately upstream of the 26mer (*CAT-EP1-G-26*, compare lanes 6 and 7). This showed increased mRNA
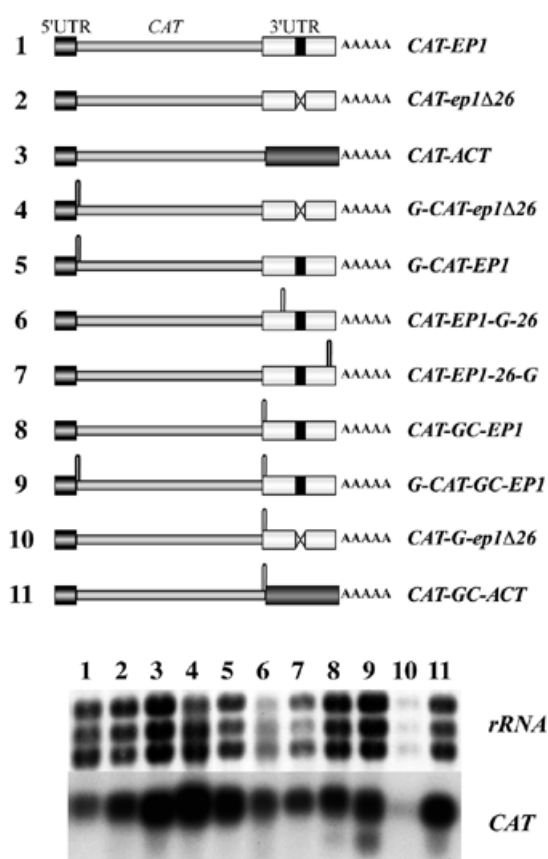
Figure 4. Contructs containing inserted secondary structures. The position of the inserted structures is indicated by the hairpin loop, and the nature of the insertions indicated in the captions. G indicates the presence of G_{30} in the mRNA, and GC indicates the presence of $G_{30}C_{30}$. A northern blot comparing steady-state *CAT* RNA levels from each cell line is shown below; lane numbers correspond to the clone numbers and the ribosomal RNA pattern (methylene blue stain) is again illustrated as a loading control above the *CAT* detection signal.

levels, half-life and CAT activity (data not shown), generally behaving as if the 26mer had been deleted. The insertion could have disrupted the secondary structure, diminishing the accessibility of the 26mer to the degradation machinery. G_{30} structures preceding the CAT coding region dimished CAT activity, presumably by inhibiting translation (not shown).

In contrast with the results obtained with both yeast and *Chlamydomonas*, no stable degradation intermediates were detected if single G_{30} structures were placed in any position. The only clear effect seen was with construct 9, which has G_{30} preceding the *CAT* gene and $G_{30}C_{30}$ between the *CAT* gene and the *EP1* 3′-UTR (*G-CAT-GC-EP1*) (Fig. 4). The most abundant mRNA was full-length, but a weaker band of ~700 nt, the size of the *CAT* gene without UTRs, was clearly present (Fig. 4, lane 9). This suggested that the RNA was subject to degradation from both ends simultaneously. If secondary structures inhibit exonucleases, but degradation is bidirectional, the insertion of a single secondary structure will give no stable intermediates. In fact, for clones 9 and 11, which have $G_{30}C_{30}$ between the *CAT* gene and either the *EP1* 3′-UTR (clone 9) or the *ACT* 3′-UTR (clone 11), a shorter band was also just perceptible on the blot shown, but the abundance was

extremely low and the band was not reproducibly detected. Construct 10, which has G_{30} between the *CAT* gene and the *ep1Δ26* 3′-UTR, never showed intermediates in any experiment. In experiments with plant and animal cells, poly(G) tracts failed to stabilise mRNA degradation intermediates, even if two tracts were included to stabilise a central portion (summarised in 53); the evidence so far suggests that plant cells must contain additional proteins (such as helicases) that can unwind secondary structures and allow digestion (53).

The result obtained with the construct containing two secondary structures indicated that *in vivo*, G_{30} could inhibit 5′→3′ exonucleases, and $G_{30}C_{30}$ could inhibit 3′→5′ exonucleases. This suggested that it might be possible to see degradation intermediates from constructs with an appropriate single secondary structure if we cut the mRNAs within the *CAT* gene. To characterise the products of 5′→3′ or 3′→5′ degradation in more detail we therefore once again subjected the mRNAs to RNase H digestion, as in Figure 3. All constructs were analysed in at least three independent experiments. The most important results are shown in Figure 5.

A diagram showing the *CAT* mRNA and the position of the different hybridisation probes used is presented in Figure 3A. Again, partial digestion products that were present in very variable amounts are marked with asterisks (above bands B and A). First, as already shown, cleavage of the *CAT-EP1* mRNA yielded three fragments. Band A represents the 3′ portion of the *CAT* gene joined to the 3′-UTR. It is shown here hybridising with the *EP1* 3′-UTR probe and the 3′ *CAT* probe. Band B contains the 5′-UTR and the 5′-portion of the *CAT* gene and is shown here hybridising with the 5′ *CAT* probe. The fragment C (centre *CAT* fragment) is not seen in Figure 5 because it did not hybridise to any of the probes used. Similar patterns were seen for *CAT-ep1Δ26* and *CAT-ACT*, except that the *CAT-ACT* of course did not hybridise with the *EP1* 3′-UTR probe. The pattern for the RNA containing G_{30} just preceding the 26mer (*CAT-ep1-G-26*) was just like that for *CAT-ep1Δ26* except that the 3′ fragment was slightly longer, as expected. The RNA with an insertion of G_{30} downstream of the 26mer (*CAT-EP1-26-G*) gave a pattern similar to *CAT-EP1*; no intermediates were seen. This could be because there is endonuclease cleavage in the 26mer, but it could also reflect an inability of the G_{30} structure to halt 3′→5′ exonucleases.

Two constructs had G_{30} inserted between the 5′-UTR and the *CAT* coding region, either with an *EP1* 3′-UTR (*G-CAT-EP1*, construct 5 in Fig. 4) or with *ep1Δ26mer* (mutant version of *EP1* 3′-UTR with deletion of regulatory 26mer sequence) 3′-UTR (5′-*G-CAT-ep1Δ26*, construct 4). These were designed to detect 5′→3′ exonuclease activity. The results are best seen on the blot hybridised with the 5′ *CAT* probe in Figure 5. In both cases, the intact 5′ portion (fragment B) was longer than for the control, as expected due to the insertion. But in addition, a fragment (D) corresponding in length to the 5′-end of the *CAT* gene without the 5′-UTR was observed. This additional fragment, which hybridised only to the *CAT* 5′ probe, could be the product of 5′→3′ exonuclease action, digesting the 5′-UTR but halting at the inserted G_{30} structure.

As could be predicted from the northern blot in Figure 4, the pattern with *CAT-GC-EP1* (construct 8), which has $G_{30}C_{30}$ between the *CAT* gene and the *EP1* 3′-UTR, also had an additional band, which is labelled E in Figures 4 and 5. The fragment was ~300 bp long and hybridised with the *CAT* 3′
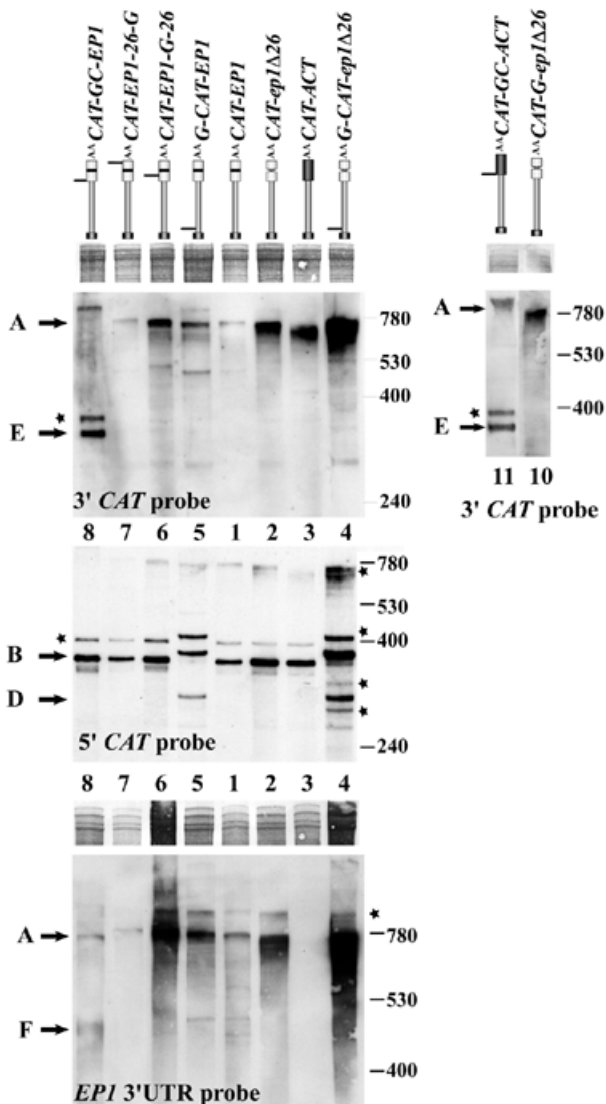
Figure 5. Identification of the degradation intermediates stabilised by secondary structures. RNA was prepared from cell lines expressing the different *CAT* mRNAs. The RNA map is above the lanes, and the clone number beneath or between the blots. RNA was digested with RNase H and separated as in Figure 3. A methylene blue stain of a portion of the gel is included to indicate the loading, and the nature of the probes used indicated on each panel. Fragments detected correspond to those illustrated in Figure 3A and asterisks again indicate partial digestion products.

probe but not with the 5′ probe or the *EP1* 3′-UTR probe (Fig. 5), indicating that it corresponded to the 3′-end of the *CAT* gene, terminating at $G_{30}C_{30}$. This could be created by 3′→5′ digestion terminating at the secondary structure. This fragment was also seen in procyclic forms, indicating that the 3′→5′ activities were active throughout the life cycle (data not shown). Similar blots of bloodstream-form mRNA hybridised with a probe specific for the *EP1* 3′-UTR showed a faint smear running at approximately the size of a (partially) deadenylated *EP1* 3′-UTR, lacking the 5′-UTR and *CAT* gene portion (fragment F in the figures). This smear was reproducible and clone-specific, so could be a product of 5′→3′ exonuclease action. A

similar construct for the *ACT* 3′-UTR containing $G_{30}C_{30}$ (construct 11) gave analogous results with the *CAT* probe, but construct 10 in which G_{30} had been inserted between the *CAT* gene and the *ep1Δ26mer*, yielded no additional bands (Fig. 5), suggesting that G_{30} was insufficient to inhibit 3′→5′ exonuclease activity in trypanosomes.

One way to confirm that these fragments represent degradation intermediates would be to perform a transcriptional pulse-chase experiment. As transcription of an mRNA was induced, the full-length RNA would increase in abundance; after transcriptional repression, the amount of full-length RNA would diminish and the abundance of intermediates would transiently increase before they too were degraded. Unfortunately this is currently not technically possible in trypanosomes. Nevertheless, we could exclude some potential artifacts, as follows. (i) The extra bands did not result from anomalous migration in the polyacrylamide gel due to strong secondary structure. This can be completely excluded for the fragment E, because it hybridised to the CAT probe but not the 3′-UTR probe. (ii) Fragment E (but not fragment D) could have been the product of transcriptional termination by T7 RNA polymerase at or just after $G_{30}C_{30}$. This was unlikely, as termination by T7 polymerase is usually very sequence specific. Nevertheless, to check, three plasmids, *CAT-GC-EP1*, *CAT-EP1* and *CAT-G-ep1Δ26*, were cleaved at a restriction site downstream of the normal polyadenylation site, and transcribed *in vitro* by T7 polymerase. Each reaction yielded a full-length band of ~1.3 kb and a smear of shorter products (not shown), but there was no evidence for specific termination at either G_{30} or $G_{30}C_{30}$. (iii) The G_{30} or $G_{30}C_{30}$ might have been targeted by RNase H or have acted as a self-cleaving ribozyme. This is again unprecedented, and can be ruled out for G_{30} as no additional band was seen with the *CAT-G-ep1Δ26* construct. To control for *in vitro* cleavage at $G_{30}C_{30}$, the *in vitro* transcripts described above were incubated under standard RNase H digestion conditions, with or without RNase H and without oligonucleotides. All products were analysed by polyacrylamide gel electrophoresis and results were again negative (not shown).

We still cannot rule out the possibility that fragments D, E and F are generated by *in vivo* T7 polymerase termination or by trypanosome endonuclease activity at the secondary structures. It is however more likely that they are products of trypanosome exonuclease action on full-length RNAs.

DISCUSSION

The results described in this manuscript suggest that constitutive mRNA degradation in trypanosomes involves gradual deadenylation followed by rapid degradation by both 5′→3′ exonucleases, as seen in yeast. The very rapid degradation induced by the U-rich 26mer instability element exhibits features consistent with either very rapid deadenylation or endonuclease cleavage.

The predominant mechanism of both regulated and constitutive mRNA degradation in yeast is deadenylation followed by decapping and 5′→3′ degradation, and a similar pathway has been described in *Chlamydomonas* (52). The principal enzyme involved in cytoplasmic 5′→3′ degradation in yeast is Xrn1p; the dependence on deadenylation is at least partially explained by the formation of a degradation complex which also includes components that can interact with the poly(A) tail (54). The

trypanosome genome database contains at least four potential homologues of Xrn1p or the similar nuclear 5′→3′ exonuclease Rat1p (H. Irmer, S. Freese and A. Estévez, unpublished results).

Yeast strains that are mutant in the deadenylation-dependent decapping pathway are viable and degrade mRNA, but at lower rates (55). Degradation now occurs in the 3′→5′ direction (56) and is effected by a complex called the exosome (57). In yeast, this degradation seems to be considerably less active than that in the 5′→3′ direction. Our results suggested that in trypanosomes 3′→5′ degradation and 5′→3′ degradation are equally active. For example, RNAs that were degraded from the 5′-end could only be detected if they were internally cleaved to create uniform 3′-termini. Failure to detect stabilised degradation intermediates by insertion of single secondary structures in mRNAs in mammalian cells has also been reported (38); this could perhaps also be due to simultaneous degradation from 3′- and 5′-ends. Trypanosomes contain several 3′→5′ exonucleases that are similar to the components of the yeast exosome, but only a subset of these are incorporated into the trypanosome exosome complex (58). It may be that the differences between the trypanosome and yeast 3′→5′ exonuclease complements, and their regulation, results in higher activity in trypanosomes. The accelerated degradation of the *EP* mRNA in trypanosomes appears to be initiated by rapid destruction of the 3′-UTR. Although a minor portion may be subject to deadenylation, the results would be more consistent with an endonuclease cleavage within the U-rich instability element. After attack on the 3′-UTR, the mRNA is digested from both ends. In order to detect any products of endonuclease cleavage, we will have to create conditional mutants in the exonuclease activities. These experiments are in progress (58).

Overall, the pattern of *EP1*-mediated mRNA decay is rather reminiscent of the regulated decay of a number of mammalian mRNAs. Degradation of some mammalian mRNAs is clearly initiated by endonuclease cleavage (32). For early response mRNAs containing AREs, there is conflicting information supporting roles for both deadenylation and endonuclease cleavage (see for example 40–42,59,60). Interestingly, AU-element-mediated decay has recently been reported in *Trypanosoma cruzi* (23), and a protein mediating the decay shows homology to mammalian proteins that regulated AU-mediated decay (61). Since many of the genes encoding the basal degradation machinery are found in trypanosomes, it is possible that the regulatory mechanisms also have ancient evolutionary origins.

REFERENCES

1. Cross,G.A.M. (1997) Antigenic variation in trypanosomes: secrets surface slowly. *Bioessays*, **18**, 283–291.

2. Roditi,I., Furger,A., Ruepp,S., Schurch,N. and Butikofer,P. (1998) Unravelling the procyclin coat of *Trypanosoma brucei. Mol. Biochem. Parasitol.*, **91**, 117–130.

3. Vanhamme,L. and Pays,E. (1995) Control of gene expression in trypanosomes. *Microbiol. Rev.*, **59**, 223–240.

4. Vanhamme,L. and Pays,E. (1998) Controls of the expression of the vsg in *Trypanosoma brucei. Mol. Biochem. Parasitol.*, **91**, 107–116.

5. Blattner,J., Helfert,S., Michels,P. and Clayton,C.E. (1998) Compartmentation of phosphoglycerate kinase in *Trypanosoma brucei* plays a critical role in parasite energy metabolism. *Proc. Natl Acad. Sci. USA*, **95**, 11596–11600.

6. Myler,P.J., Audleman,L., deVos,T., Hixson,G., Kiser,P., Lemley,C., Magness,C., Rickel,E., Sisk,E., Sunkin,S., Swartzell,S., Westlake,T., Bastien,P., Fu,G., Ivens,A. and Stuart,K. (1999) *Leishmania major* Friedlin chromosome 1 has an unusual distribution of protein-coding genes. *Proc. Natl Acad. Sci. USA*, **96**, 2902–2906.

7. Matthews,K.R., Tschudi,C. and Ullu,E. (1994) A common pyrimidine-rich motif governs *trans*-splicing and polyadenylation of tubulin polycistronic pre-mRNA in trypanosomes. *Genes Dev.*, **8**, 491–501.

8. Schürch,N., Hehl,A., Vassella,E., Braun,R. and Roditi,I. (1994) Accurate polyadenylation of procyclin mRNAs in *Trypanosoma brucei* is determined by pyrimidine-rich elements in the intergenic regions. *Mol. Cell. Biol.*, **14**, 3668–3675.

9. Hug,M., Hotz,H.R., Hartmann,C. and Clayton,C.E. (1994) Hierarchies of RNA processing signals in a trypanosome surface antigen mRNA precursor. *Mol. Cell. Biol.*, **14**, 7428–7435.

10. Pasion,S.G., Hines,J.C., Ou,X., Mahmood,R. and Ray,D.S. (1996) Sequences within the 5′ untranslated region regulate the levels of a kinetoplast DNA topoisomerase mRNA during the cell cycle. *Mol. Cell. Biol.*, **16**, 6724–6735.

11. Clayton,C. and Hotz,H.-R. (1996) Post-transcriptional control of PARP gene expression. *Mol. Biochem. Parasitol.*, **77**, 1–6.

12. Hotz,H.-R., Biebinger,S., Flaspohler,J. and Clayton,C.E. (1998) *PARP* gene expression: regulation at many levels. *Mol. Biochem. Parasitol.*, **91**, 131–143.

13. Aly,R., Argaman,M., Halman,S. and Shapira,M. (1994) A regulatory role for the 5′ and 3′ untranslated regions in differential expression of hsp83 in *Leishmania. Nucleic Acids Res.*, **22**, 2922–2929.

14. Argaman,M., Aly,R. and Shapira,M. (1994) Expression of the heat shock protein 83 in *Leishmania* is regulated post-transcriptionally. *Mol. Biochem. Parasitol.*, **64**, 95–110.

15. Blattner,J. and Clayton,C.E. (1995) The 3′-untranslated regions from the *Trypanosoma brucei* phosphoglycerate kinase genes mediate developmental regulation. *Gene*, **162**, 153–156.

16. Häusler,T. and Clayton,C.E. (1996) Post-transcriptional control of hsp 70 mRNA in *Trypanosoma brucei. Mol. Biochem. Parasitol.*, **76**, 57–72.

17. Hotz,H.-R., Lorenz,P., Fischer,R., Krieger,S. and Clayton,C.E. (1995) Developmental regulation of hexose transporter mRNAs in *Trypanosoma brucei. Mol. Biochem. Parasitol.*, **75**, 1–14.

18. Charest,H., Zhang,W.-W. and Matlashewski,G. (1996) The developmental expression of *Leishmania donovani* A2 amastigote-specific genes is post-transcriptionally mediated and involves elements in the 3′-untranslated region. *J. Biol. Chem.*, **271**, 17081–17090.

19. Teixeira,S.M.R., Kirchhoff,L.V. and Donelson,J.E. (1995) Post-transcriptional elements regulating expression of mRNAs from the amastin/tuzin gene cluster of *Trypanosoma cruzi. J. Biol. Chem.*, **270**, 22586–22594.

20. Nozaki,T. and Cross,G.A.M. (1995) Effects of 3′-untranslated and intergenic regions on gene expression in *Trypanosoma cruzi. Mol. Biochem. Parasitol.*, **75**, 55–68.

21. Berberof,M., Vanhamme,L., Tebabi,P., Pays,A., Jefferies,D., Welburn,S. and Pays,E. (1995) The 3′-terminal region of the mRNAs for VSG and procyclin can confer stage specificity to gene expression in *T. brucei. EMBO J.*, **14**, 2925–2934.

22. Hotz,H.-R., Hartmann,C., Huober,K., Hug,M. and Clayton,C.E. (1997) Mechanisms of developmental regulation in *Trypanosoma brucei*: A polypyrimidine tract in the 3′-untranslated region of a trypanosome surface protein mRNA affects RNA abundance and translation. *Nucleic Acids Res.*, **25**, 3017–3025.

23. Di Noia,J.M., D'Orso,I., Sánchez,D.O. and Frasch,A.C.C. (2000) AU-rich elements in the 3′-untranslated region of a new mucin-type gene family of *Trypanosoma cruzi* confers mRNA instability and modulates translation efficiency. *J. Biol. Chem.*, **275**, 10218–10227.

24. Biebinger,S., Rettenmaier,S., Flaspohler,J., Hartmann,C., Peña-Diaz,J., Wirtz,L.E., Hotz,H.R., Barry,J.D. and Clayton,C.E. (1996) The PARP promoter of *Trypanosoma brucei* is developmentally regulated in a chromosomal context. *Nucleic Acids Res.*, **24**, 1202–1211.

25. Navarro,M., Cross,G.A.M. and Wirtz,E. (1999) *Trypanosoma brucei* variant surface glycoprotein regulation involves coupled activation/inactivation and chromatin remodeling of expression sites. *EMBO J.*, **18**, 2265–2272.

26. Horn,D. and Cross,G.A.M. (1997) Position-dependent and promoter-specific regulation of gene expression in *Trypanosoma brucei*. *EMBO J.*, **16**, 7422–7431.

27. Roditi,I. and Clayton,C.E. (1999) An unambiguous nomenclature for the major surface glycoprotein genes of the procyclic form of *Trypanosoma brucei*. *Mol. Biochem. Parasitol.*, **103**, 99–100.

28. Hehl,A., Vassella,E., Braun,R. and Roditi,I. (1994) A conserved stem-loop structure in the 3′ untranslated region of procyclin mRNAs regulates expression in *Trypanosoma brucei*. *Proc. Natl Acad. Sci. USA*, **91**, 370–374.

29. Furger,A., Schürch,N., Kurath,U. and Roditi,I. (1997) Elements in the 3′ untranslated region of procyclin mRNA regulate expression in insect forms of *Trypanosoma brucei* by modulating RNA stability and translation. *Mol. Cell. Biol.*, **17**, 4372–4380.

30. Drozdz,M. and Clayton,C.E. (1999) Structure of a regulatory 3′-untranslated region from *Trypanosoma brucei*. *RNA*, **5**, 1632–1644.

31. Decker,C.J. and Parker,R. (1993) A turnover pathway for both stable and unstable mRNAs in yeast: evidence for a requirement for deadenylation. *Genes Dev.*, **7**, 1632–1643.

32. Mitchell,P. and Tollervey,D. (2000) mRNA stability in eucaryotes. *Curr. Opin. Genet. Dev.*, **10**, 193–198.

33. Körner,C.G., Wormington,M., Muckenthaler,M., Schneider,S., Dehlin,E. and Wahle,E. (1998) The deadenylating nuclease (DAN) is involved in poly(A) tail removal during the meiotic maturation of *Xenopus* oocytes. *EMBO J.*, **17**, 5427–5437.

34. Bashkirov,V.I., Scherthan,H., Solinger,J.A., Buerstedde,J.M. and Heyer,W.D. (1997) A mouse cytoplasmic exoribonuclease (mXRN1p) with preference for G4 tetraplex substrates. *J. Cell Biol.*, **136**, 761–773.

35. Shiomi,T., Fukushima,K., Suzuki,N., Nakashima,N., Noguchi,E. and Nishimoto,T. (1998) Human dis3p, which binds to either GTP- or GDP-Ran, complements *Saccharomyces cerevisiae dis3*. *J. Biochem.*, **123**, 883–890.

36. Binder,R., Horowitz,J.A., Basilion,J.P., Koeller,D.M., Klausner,R.D. and Harford,J.B. (1994) Evidence that the pathway of transferrin receptor mRNA degradation involves an endonucleolytic cleavage within the 3′-UTR and does not involve poly(A) tail shortening. *EMBO J.*, **13**, 1969–1980.

37. Wang,Z. and Kiledjian,M. (2000) Identification of an erythroid-enriched endoribonuclease activity involved in specific mRNA cleavage. *EMBO J.*, **19**, 295–305.

38. Curatola,A.M., Nadal,M.S. and Schneider,R.J. (1995) Rapid degradation of AU-rich element (ARE) mRNAs is activated by ribosome transit and blocked by secondary structure at any position 5′ to the ARE. *Mol. Cell Biol.*, **15**, 6331–6340.

39. Peng,S.S., Chen,C.Y. and Shyu,A.B. (1996) Functional characterization of a non-AUUUA AU-rich element from the c-jun proto-oncogene mRNA: evidence for a novel class of AU-rich elements. *Mol. Cell Biol.*, **16**, 1490–1499.

40. Peng,S.S., Chen,C.Y., Xu,N. and Shyu,A.B. (1998) RNA stabilization by the AU-rich element binding protein, HuR, an ELAV protein. *EMBO J.*, **17**, 3461–3479.

41. Fan,X.C. and Steitz,J.A. (1998) Overexpression of HuR, a nuclear-cytoplasmic shuttling protein, increases the *in vivo* stability of ARE-containing mRNAs. *EMBO J.*, **17**, 3448–3460.

42. Zhao,Z., Chang,F.-C. and Furneaux,H.M. (2000) The identification of an endonuclease that cleaves within an HuR binding site in mRNA. *Nucleic Acids Res.*, **28**, 2695–2701.

43. Dorn,P.L., Aman,R.A. and Boothroyd,J.C. (1991) Inhibition of protein synthesis results in super-induction of procyclin (PARP) RNA levels. *Mol. Biochem. Parasitol.*, **44**, 133–140.

44. Graham,S.V. and Barry,J.D. (1996) Polysomal, procyclin mRNAs accumulate in bloodstream forms of monomorphic and pleomorphic trypanosomes treated with protein synthesis inhibitors. *Mol. Biochem. Parasitol.*, **80**, 179–192.

45. Schürch,N., Furger,A., Kurath,U. and Roditi,I. (1997) Contribution of the procyclin 3′ untranslated region and coding region to the regulation of expression in bloodstream forms of *Trypanosoma brucei*. *Mol. Biochem. Parasitol.*, **89**, 109–121.

46. Wirtz,L.E., Hartmann,C. and Clayton,C.E. (1994) Gene expression mediated by bacteriophage T3 and T7 RNA polymerases in transgenic trypanosomes. *Nucleic Acids Res.*, **22**, 3887–3894.

47. Wirtz,E., Hoek,M. and Cross,G.A.M. (1998) Regulated processive transcription of chromatin by T7 RNA polymerase in *Trypanosoma brucei*. *Nucleic Acids Res.*, **26**, 4626–4634.

48. Brittingham,A., Miller,M.A., Donelson,J.E. and Wilson,M.E. (2001) Regulation of GP63 mRNA stability in promastigotes of virulent and attenuated *Leishmania chagasi*. *Mol. Biochem. Parasitol.*, **112**, 51–59.

49. Wirtz,L.E. and Clayton,C.E. (1995) Inducible gene expression in trypanosomes mediated by a procaryotic repressor. *Science*, **268**, 1179–1183.

50. Irmer,H. (2001) mRNA-degradation in *Trypanosoma brucei*. PhD thesis, University of Heidelberg, Germany.

51. Muhlrad,D., Decker,C.J. and Parker,R. (1994) Deadenylation of the unstable mRNA encoded by the yeast MFA2 gene leads to decapping followed by 5′-3′ digestion of the transcript. *Genes Dev.*, **8**, 855–866.

52. Gera,J.F. and Baker,E.J. (1998) Deadenylation-dependent and -independent decay pathways for alpha1-tubulin mRNA in *Chlamydomonas reinhardtii*. *Mol. Cell. Biol.*, **18**, 1498–1505.

53. Kastenmeier,J.P. and Green,P.J. (2000) Novel features of the XRN-family in *Arabidopsis*: evidence that ATXRN4, one of several orthologs of nuclear Xrn2p/rat1p, functions in the cytoplasm. *Proc. Natl Acad. Sci. USA*, **97**, 13985–13990.

54. Bouveret,E., Rigaut,G., Shevchenko,A., Wilm,M. and Séraphin,B. (2000) A Sm-like protein complex that participates in mRNA degradation. *EMBO J.*, **19**, 1661–1671.

55. Beelman,C.A. and Parker,R. (1995) Degradation of mRNA in eukaryotes. *Cell*, **81**, 179–184.

56. Muhlrad,D., Decker,C.J. and Parker,R. (1995) Turnover mechanisms of the stable yeast PGK1 mRNA. *Mol. Cell. Biol.*, **15**, 2145–2156.

57. Jacobs-Anderson,J.S. and Parker,R.P. (1998) The 3′ to 5′ degradation of yeast mRNAs is a general mechanism for mRNA turnover that requires the SKI2 DEVH box protein and 3′ to 5′ exonucleases of the exosome complex. *EMBO J.*, **17**, 1497–1506.

58. Estévez,A., Kempf,T. and Clayton,C.E. (2001) The exosome of *Trypanosoma brucei*. *EMBO J.*, **20**, 3831–3839.

59. Chen,C.Y., Xu,N. and Shyu,A.B. (1995) mRNA decay mediated by two distinct AU-rich elements from c-fos and granulocyte-macrophage colony-stimulating factor transcripts: different deadenylation kinetics and uncoupling from translation. *Mol. Cell Biol.*, **15**, 5777–5788.

60. Voeltz,G.K. and Steitz,J.A. (1998) AUUUA sequences direct mRNA deadenylation uncoupled from decay during *Xenopus* early development. *Mol. Cell. Biol.*, **18**, 7537–7545.

61. D'Orso,I. and Frasch,A.C.C. (2001) TcUBP-1, a developmentally regulated U-rich RNA-binding protein involved in selective mRNA destabilization in trypanosomes. *J. Biol. Chem.*, **276**, 34801–34809.